

## Chapter 2

# Extracellular Matrix Dynamics in Early Development

Andras Czirok, Brenda J. Rongish, and Charles D. Little

**Abstract** The extracellular matrix (ECM) is an inherently dynamic structure during development. Large-scale tissue movements sweep the ECM to distant positions during early embryogenesis; furthermore, the previously assembled ECM filaments are extensively reused during later organogenesis. Thus, some organs, such as the heart, inherit previously assembled ECM filaments. This review focuses on the macro-assembly dynamics of fibronectin and fibrillin-2 in avian embryos. Both ECM proteins are ubiquitous in vertebrate embryos at the earliest stages of development. Recent studies compared the movement of these two ECM components and suggested that the ECM moves as a composite material, whereby distinct molecular components as well as spatially separated layers exhibit similar displacements. Utilizing advances in microscopy and high-resolution particle image velocimetry algorithms, two ECM filament relocation processes can be distinguished—each operating on different length scales. First, ECM filaments are moved by large-scale tissue motion, which rearranges major organ primordia within the embryo. The second type of motion, on the scale of the individual ECM filaments, is driven by local motility and protrusive activity of nearby cells. Both kinds of motion contribute substantially to the establishment of normal ECM structure, and both must be taken into account when attempting to understand ECM macro-assembly during embryonic morphogenesis. ECM filaments also fluctuate locally—likely reflecting pulsatile cell contractility in the associated tissues. Suppression of these fluctuations by temporal averaging yields a persistent movement pattern that is shared among embryos at equivalent stages of development.

---

A. Czirok (✉)

Department of Anatomy and Cell Biology, University of Kansas Medical Center, 3901 Rainbow Blvd., Kansas City, KS 66160, USA

Department of Biological Physics, Eotvos University, Budapest, Hungary

e-mail: [aczirok@kumc.edu](mailto:aczirok@kumc.edu)

B.J. Rongish • C.D. Little

Department of Anatomy and Cell Biology, University of Kansas Medical Center, 3901 Rainbow Blvd., Kansas City, KS 66160, USA

Recent studies comparing the motion of embryonic mesenchymal cell populations (newly ingressed mesodermal, pre-somitic, endothelial, and endocardial) all found that the gross displacement of these cells is to a large extent shared by the surrounding ECM. The result being that active motion relative to the local ECM scaffold is more random than previously appreciated. A future understanding of ECM assembly thus requires the study of the complex interactions between biochemical assembly steps, local cell action and the biomechanics of tissue motion.

## 2.1 Introduction

In addition to providing structure to the interstitial spaces between cells, the ECM acts as a scaffold for cell adhesion. This contact mediates cell migration (movement relative to the ECM) and also allows the cells to exert mechanical forces. Cell binding to the ECM can elicit signal transduction events across the cell plasma membrane (Alberts et al. 2008). The ECM is also believed to play a biochemical and/or biomechanical role in the specification of cell fate. Since ECM constituents bind and sequester soluble growth factors, the ECM can modulate—either restrict or promote—access of ligands to specific cell surface receptors. Thus, the ECM is positioned to regulate the spatial and temporal localization of most growth factors after their secretion. Such ECM-bound growth factors may also stimulate directional cell migration through chemotaxis (Yang et al. 2002; Vasiev et al. 2010). Mechanical cues from the microenvironment are also likely transmitted through ECM–integrin interactions and modulate intracellular signaling and gene expression patterns. For example, the degree of ECM stiffness contributes to cell fate determination of mesenchymal stem cells (Engler et al. 2006). Thus, the local ECM environment can influence cell polarity, survival, proliferation, and differentiation (Rozario and DeSimone 2010).

Although the ECM is a composite structure made up of many different constituents, the three-dimensional (3D) organization of the ECM can be as crucial as its molecular composition in determining its developmental functions. Cellular response to ECM contacts strongly depends on how the ECM is presented to cell surface receptors *in vitro*: whether it is immobilized, planar, or three-dimensional (Zamir et al. 1999; Cukierman et al. 2001). ECM organization also strongly influences cell shape and motility (Tomasek et al. 1982; Petroll and Ma 2003): Fibroblasts (Stoplak and Harris 1982; Dickinson et al. 1994), endothelial cells (Vernon et al. 1995), and neurons (Dubey et al. 2001) are all known to preferentially follow oriented fibers. At the tissue level of organization, mechanical properties, such as anisotropy or load bearing capacity, are determined by 3D ECM structure (Barocas and Tranquillo 1997; Olsen et al. 1999).

The experimental accessibility of avian embryos makes them especially suitable as model organisms in which to study ECM organization during development (Rongish et al. 1998; Czirok et al. 2004, 2006b). Two ECM components, fibronectin and fibrillin-2, were found to be especially fruitful targets of investigations: Both

can be labeled *in vivo* by high-affinity antibodies, and both proteins assemble into large, characteristic structures spanning tens of micrometers. During day 1 of gestation, a rich 3D ECM structure is readily apparent. Bundles of fibrillin fibers connect the posterior foregut (anterior intestinal portal, AIP) to the somitic regions, extending well past the first few somite pairs. In addition there are prominent coaxial fibrillin-2 fibers that assemble parallel to the (future) vertebral axis. The cranial portion of these bundles encloses the somites, while caudally the bundles extend more than 200  $\mu\text{m}$  into the segmental plate mesoderm and approach Hensen's node (organizer). Caudal to the node, fibrillin-2 exhibits a strikingly different pattern, which consists of punctate, disconnected foci. The somitic array and the segmental plate mesoderm exhibit an oriented, dense array of paraxial filaments, remarkably different from the loose meshwork-like organization characteristic of the more lateral embryonic regions. In contrast, fibronectin exhibits a finer meshwork-like pattern, with less variability across the lateral plate. Yet, despite these differences, at the resolution of confocal microscopy, most ECM filaments are composite structures containing both proteins (Fig. 2.1).

## 2.2 ECM Dynamics

### 2.2.1 Labeling Technique

In order to study ECM dynamics, its constituent proteins can be conveniently labeled in avian embryos by the microinjection of fluorochrome-conjugated monoclonal antibodies, such as JB3, a monoclonal IgG that binds avian fibrillin-2 (Rongish et al. 1998), or B3D6, which recognizes avian fibronectin (Gardner and Fambrough 1983). After antibody microinjection at Hamburger and Hamilton (HH) stages 4–7 (Hamburger and Hamilton 1951), embryos can be recorded for several hours with automated microscopy (Czirok et al. 2002). During the recordings no substantial photo bleaching or other signal deterioration is obvious (Fig. 2.2).

After microinjection, antibodies infiltrate a substantial portion (up to 50–70 %) of the area pellucida in less than an hour. Injection of living avian embryos with ECM antibodies has been in use for over 15 years (Little and Drake 2000). The perturbative effect of microinjected antibodies was assayed by comparing whole-mounted antibody-injected embryos to non-injected controls after 10 h of development. No observable differences were found either in the post-fixation ECM staining pattern or in the anatomy of the embryos. The timing of major morphogenic processes was also the same in antibody-injected embryos and non-injected controls. In particular, the somites form on identical schedules, every 90 min, while the heart loops and commences beating normally (Czirok et al. 2004).

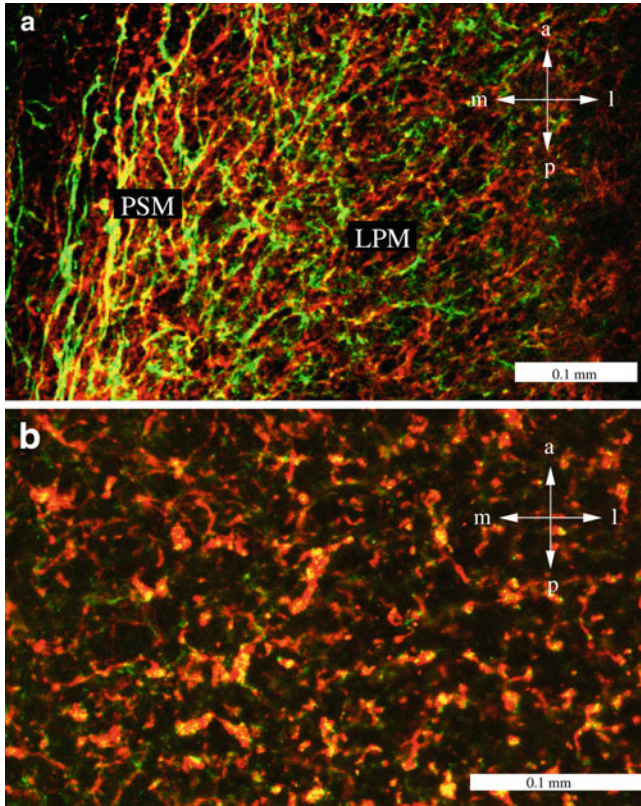


**Fig. 2.1** Confocal images of fibronectin (*red*) and fibrillin-2 (*green*) in a 4-somite (Hamburger and Hamilton stage 7) embryo. The images depict a dorsal–ventral (*z*) projection of the ECM layer located between the mesoderm and the endoderm. Panel **a** shows the ECM associated with the pre-somitic and lateral plate mesoderm. Long fibrillin-2 rich filaments running parallel to the anterior–posterior axis are abundant around the pre-somitic mesoderm. Panel **b** shows an area lateral to the primitive streak. ECM filaments are much shorter and are oriented in random directions. Co-localization of the two ECM components appears as *yellow*. Images were obtained using a  $25\times$  oil immersion objective and a Zeiss LSM510 confocal microscope. *a* anterior, *p* posterior, *m* medial, *l* lateral, *PSM* pre-somitic mesoderm, *LPM* lateral plate mesoderm

### 2.2.2 Large-Scale ECM Flow Pattern

As reported in Czirok et al. (2004), the fluorescence staining pattern of the ECM changes remarkably during a recording period of 8–12 h (Fig. 2.2). Yet, filament shapes and their relative positions remain fairly similar between consecutive image pairs (separated by 5–10 min intervals)—a feature that makes our tracking procedure possible. In fact, filament motion seems to be as ordered as the slow flow of a viscous fluid: Adjacent filaments move on parallel trajectories.

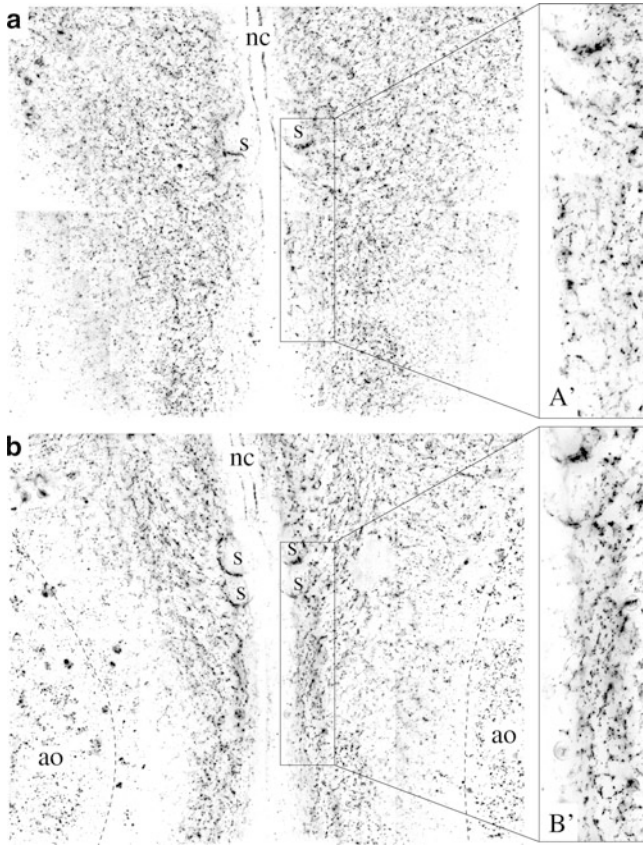


**Fig. 2.2** Fibronectin, as visualized by microinjected and fluorophore-conjugated B3D6 antibodies at the beginning of a recording (**a**) and 4 h later (**b**). Images were obtained with a  $10\times$  objective in a widefield setting, subjected to a blind deconvolution to reduce out-of-focus blur; grayscale values were inverted to increase contrast and aid visualization. The pre-somitic mesoderm and the somites are shown at higher magnification in panels **a'** and **b'**. Notice the increased density of fibronectin filaments surrounding the pre-somitic mesoderm, a consequence of the large-scale ECM motion during the observed time period. The *boxes* are  $200\ \mu\text{m}$  wide. *ao* area opaca, *nc* notochord, *s* somite

ECM displacements are extracted either by a manual frame-by-frame tracking procedure (Czirok et al. 2004) or by an automatic pattern-matching algorithm [PIV; Zamir et al. (2005)]. The latter method divides the image into small image tiles. For each tile the algorithm scans the next frame for the image detail of the same size that is most similar to the given tile of the previous frame. The spatial shift between the best matching pattern and the original tile gives an estimate for the displacement of the objects within the tile. During either the manual or the automatic PIV procedures, images are registered in such a way that the somites remain stationary—thus, all motion data are presented in a reference system co-moving with the somites.



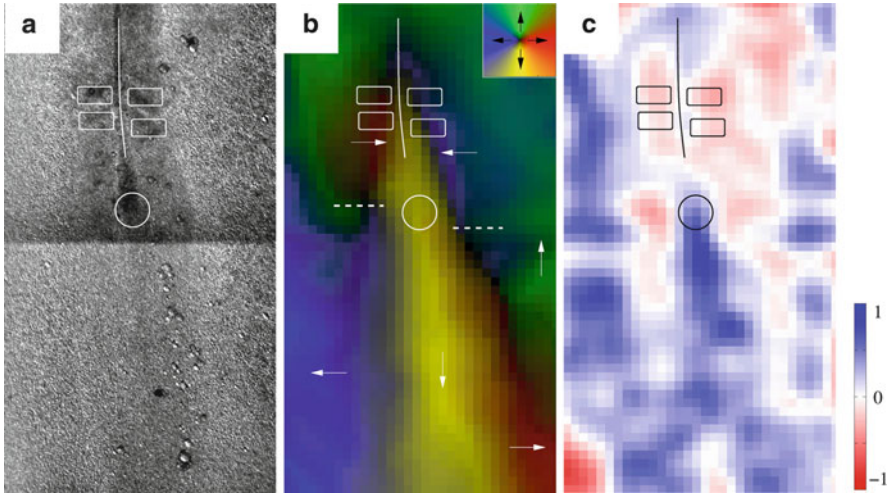


**Fig. 2.3** ECM motion pattern in a two-somite (Hamburger and Hamilton stage 6) embryo. (a) A ventral view of embryo morphology, visualized by DIC optics. Anatomical features such as somites, the notochord, and Hensen's node are marked with *boxes*, a *vertical line*, and a *circle*, respectively. (b) Magnitude and directionality of the persistent ECM movement pattern, represented by intensity and color as shown in the inset. *Arrows* indicate motion direction at selected positions to aid the reader in perceiving motion patterns. *Dashed lines* mark the boundary between the medially and laterally moving regions of the lateral plate mesoderm. (c) Accumulation (*red*) or dilution (*blue*) of ECM filaments, calculated from the divergence of the ECM velocity field. The rate of the motion-related increase in ECM density can be substantial; the unit of the scale corresponds to a change of 100 %/h. After Szabo et al. (2011)

The ECM motion pattern can be extracted either by averaging over multiple stage-matched specimens (Czirok et al. 2004) or by averaging over several frame pairs in the case of a single specimen (Szabo et al. 2011). Displacement patterns obtained by either averaging method are highly reproducible. Convergent-extension-like anatomical movements take place lateral to the notochord. Hensen's node and the primitive streak move caudally, and the head region extends cranially. During this period of cranio-caudal axis extension, the ECM surrounding the lateral plate mesoderm (LPM) moves medially. In the caudal embryo, near the primitive streak, the LPM-associated ECM moves laterally. The combination of these displacements results in a vortex-like motion pattern on both the right and left sides of the embryo. The region where the ECM converges medially elongates over progressively later stages of development. The moving boundary separating medial convergence from the more caudal domain, characterized by lateral expansion, is often asymmetric: The domain of medialward movement is larger on the right side of the acquired image frame (the anatomical left side of the embryo). Thus, lateral expansion takes place only at more caudal positions (see dashed lines in Fig. 2.3). This left-right asymmetry in ECM movements around Hensen's node complements recent results, indicating the rotation of cellular components of the node in avians (Cui et al. 2009; Gros et al. 2009).

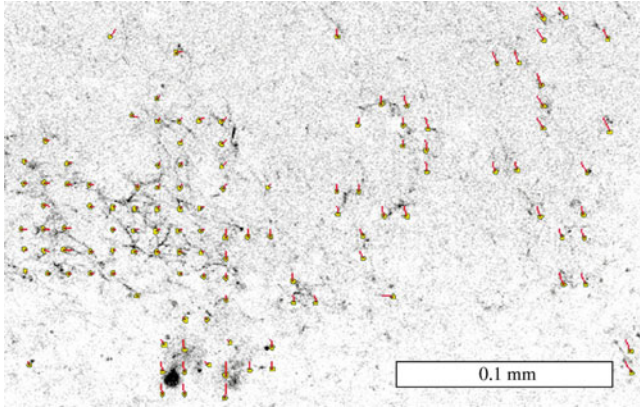


**Fig. 2.4** Fluctuating movements of fibrillin-2 filaments, assessed by confocal microscopy. A single,  $0.7\ \mu\text{m}$  thick optical plane is shown, with the estimated velocity vectors superimposed. *Red lines* indicate the calculated displacements of the *yellow dots*. As the ECM layer separating the mesoderm from the endoderm is not perfectly flat, only an irregular area within the optical section contains high ECM density. The motion is locally smooth, but varies in direction and magnitude over a scale of  $100\ \mu\text{m}$ . After Szabo et al. (2011)

The obtained speeds of ECM movements can exceed  $100\ \mu\text{m}/\text{h}$ , fast enough to substantially reorganize ECM distribution within a few hours. The observed movements are shared by two distinct ECM components, fibronectin and fibrillin-2. In particular, the cross-correlation coefficient of the simultaneous displacements of fibronectin and fibrillin-2 is 0.91 (Szabo et al. 2011). Similar ECM movements are also present during epithelial tissue morphogenesis in the ancient metazoan, *Hydra* (Aufschnaiter et al. 2011).

### 2.2.3 *Fluctuations*

Surprisingly, velocity field snapshots of ECM movements show considerable variability in the absence of averaging (Szabo et al. 2011). We attribute this phenomenon to intrinsic fluctuations within the tissue. The magnitude and the spatial extent of the fluctuations are somewhat smaller, but comparable to that of the persistent motion pattern. The fluctuations, however, change rapidly: High-frame-rate confocal scans indicated that the correlation time of the fluctuations is, despite their large spatial extent, less than a minute. The fluctuations result in local contractions and expansions of the ECM at apparently random locations (Fig. 2.4), which are similarly short-lived and which lack an obvious correlation with anatomical structures.

The long spatial correlation length (large extent of co-moving area) of the fluctuations is consistent with the idea that the tissue is in mechanical equilibrium; therefore, a local change in cell-generated mechanical forces is expected to

immediately alter tissue deformations elsewhere. Recent studies in fly embryos described a pulsatile, ratchet-like contraction mechanism (Martin et al. 2009). Instead of a uniformly distributed contractile activity spread across the tissue, individual cells were observed to undergo a repeating cycle of asynchronous contractions, with cytoskeletal stiffening followed by relaxation and physical rearrangements. A mechanism similar to that in the fly might explain the ECM fluctuations we observe—however, it is unclear how these pulsatile cycles might be generated in bird embryos or how such fluctuations might affect the large-scale ECM displacements we observe during amniote morphogenesis.

## 2.3 ECM Restructuring

### 2.3.1 *Remodeling*

The observed large-scale ECM movements have a profound impact on tissue scale architecture. As an example, the bundles of ECM filaments that run parallel to the embryonic axis in the vicinity of the pre-somitic mesoderm are formed by these movements. The filaments are assembled from smaller ECM fibrils, units that were previously scattered over an extended area. The medial movement of these nascent ECM filaments, accompanied by stretching along the embryonic axis, both orients and condenses the ECM filaments into larger caliber coaxial cables (Czirok et al. 2004).

Similarly, a substantial component of the future cardiac jelly ECM is drawn from the LPM. A recent study determined that the anatomical origin of ECM filaments that eventually contribute to the developing heart tube can be mapped (Aleksandrova et al. 2012). Extensive tracing of fluorescently labeled endogenous and exogenous fibronectin filaments revealed that (1) ECM flanking the foregut region (AIP) in HH stage 8 embryos contributes to the anterior third of the heart tube, (2) areas located lateral to the caudal segments of the anterior zone, on both sides, are the source of ECM fibrils that are eventually translocated to the middle portion of the cardiac tube, and (3) moving tailward, the region contributing ECM to the caudal heart tube and omphalomesenteric veins maps to the posterior end of the foregut and extends caudally to the level of the second or third somite pair at HH stage 8.

These time-resolved positional mapping data show that preexisting ECM structures are extensively displaced and reused during development. Thus, it is now meaningful to discuss ECM positional fate, in a manner similar to the establishment of fate maps for cell populations. Interestingly, no ECM disassembly was ever observed within our sample of more than 200 recorded embryos.



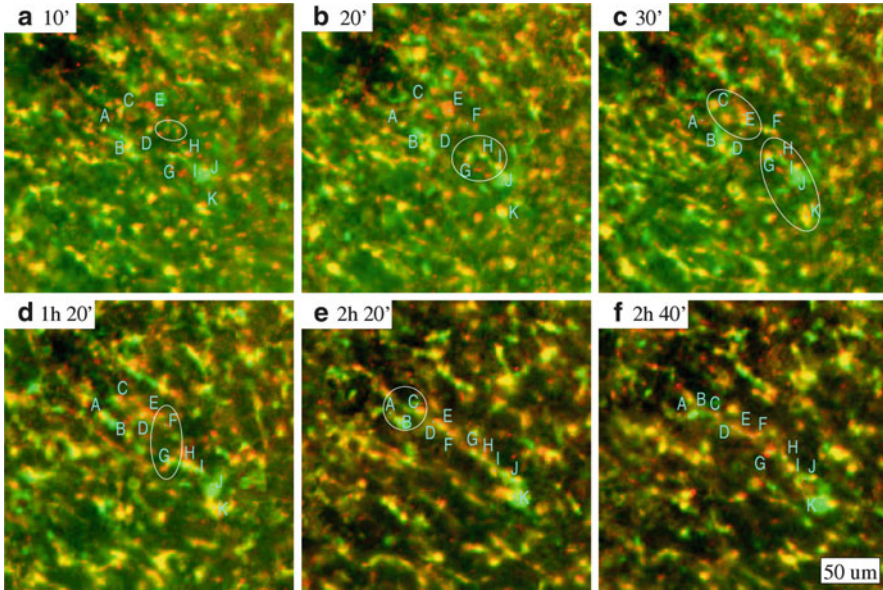


**Fig. 2.5** ECM macro-assembly, in vivo. The image sequence depicts a region of interest (ROI) located lateral to the primitive streak. The ROI is moving with the surrounding tissue. Letters denote individual globules of ECM material, which typically contain both fibronectin (red) and fibrillin-2 (green). In the course of 3 h, the globules assume an ordered, linear shape, which remains stable until the end of observation, 7 h later (not shown). *Ellipses* indicate areas where previously distinct ECM objects merge and are subsumed into a stable linear arrangement. As an example, the filament marked by F in panel (b) is created from the material enclosed in the *white ellipse* in panel (a). After Czirok et al. (2006b)

### 2.3.2 Filament Assembly

A particularly interesting reorganization process, filament assembly, can be observed to proceed in the caudal avian embryo, near the primitive streak/organizer region (Czirok et al. 2006b). ECM filaments that originally appear as globular patches of fluorescence coalesce into larger linear structures (Fig. 2.5). Closer analysis reveals that the process appears to be hierarchical, whereby elongated larger caliber structures are created by the aggregation of smaller units. Throughout the assembly process, participating ECM filaments appear to consist of both fibronectin and fibrillin-2; thus, at the level of resolution in our studies (1  $\mu\text{m}$ ), filaments are “born” as composite structures. A similar hierarchical assembly process was observed in densely populated cell cultures, where the ECM is assembled first into distinct globules on the cell surface; this was followed by the appearance of progressively larger filaments which appeared to be organized by the motile activity of several adjacent cells. Thus, when viewed in time-lapse, local cellular behavior appeared to organize ECM assemblies (Czirok et al. 2006a; Kozel et al. 2006; Sivakumar et al. 2006). Similar processes are observed in the caudal

avian embryo with the added complexity that there are long-range tissue displacements occurring concomitant with cell shape change and local motile activity.

## 2.4 ECM as a Microenvironment for Mesenchymal Cell Migration

### 2.4.1 *Methods to Visualize Cell Motion Relative to the ECM Environment*

To compare cellular displacements to that of the local ECM scaffold, simultaneous recordings are required of both the labeled ECM and cell populations. As we discussed in Sect. 2.1, the ECM is conveniently visualized by microinjected, fluorophore-conjugated antibodies. To visualize a specific cell population, one can rely on the same immunolabeling method using antibodies directed against specific cell surface epitopes. Lipophilic dyes that bind to the cell membrane or dyes taken up by the cells can be also administered locally. Transfection and electroporation of fluorescent protein-expressing constructs have also been used to target and label cell populations (Cui et al. 2006). Recently, transgenic quail strains have been developed with promising new possibilities for the visualization of cell and tissue behavior in a live amniote embryo (Sato et al. 2010).

The movement of mesodermal or other mesenchymal cells relative to the local ECM environment is defined using the vector relation of velocity addition:

$$\underbrace{d'_{\text{cell}}}_{\text{total cell displacement}} = \underbrace{d'_{\text{ECM}}}_{\text{ECM displacement at the cell's location}} + \underbrace{d'_{\text{active}}}_{\text{displacement due to active cell motility}}. \quad (2.1)$$

Thus, if both cells and ECM components can be traced at the same location, the difference between the two displacement vectors is attributed to active cell motion. Definition (2.1) is consistent with the various ways cell motility is studied. In most two- and three-dimensional in vitro settings, like invasion into collagen gels, the ECM environment is static ( $d_{\text{ECM}} = 0$ ); hence, all observed cell displacements are due to active cell motility. Furthermore, relation (2.1) ensures that passive objects ( $d_{\text{active}} = 0$ ) move similarly to the ECM—a physical characteristic experimentally verified by tracking injected microbeads into the lateral heart forming fields of quail embryos (Aleksandrova et al. 2012).

It is important to note that relation (2.1) focuses on active cell movements that use the “classical” motility apparatus, which relies upon binding and release of cell–ECM contact points to move the cell body forward (relative to the ECM) (Lauffenburger and Horwitz 1996; Ridley et al. 2003). Other, less understood

cellular activities, such as motility using cell–cell contacts—sometimes referred to as intercellular motility (Gumbiner 2005)—may also result in cell displacements. As reviewed in Montell (2008), germ-band elongation in *Drosophila* is resulted by a repeating cycle consisting of cellular contraction along the lateral direction and modulation of cell–cell adhesion. In this process contacts between two cells that are located parallel to the anterior–posterior axis are gradually replaced with new contacts between cells that are lined up along the perpendicular (lateral) direction. Thus, intercalation progresses because cell–neighborhood relationships and cell–cell contacts are spatially reorganized in the plane of the epithelium following an ordered pattern of disassembly and reassembly (Bertet et al. 2004). If cells are engaged in a motile activity where they get traction not from the ECM but from the epithelial neighbors, then this activity can be the driving force behind the co-movement of an epithelial sheet and the surrounding ECM.

To employ the above definition (2.1), one needs to establish ECM displacement in the cell's immediate vicinity. This is either readily available from co-tracing adjacent cells and ECM filaments, or must be estimated. As we discussed in Sect. 2.2, ECM displacements are very similar at locations that are sufficiently near one another; thus, a general estimate of ECM displacement is made possible by interpolating from displacement vectors obtained from suitably close locations. In our analysis we interpolate data within a radius of 5  $\mu\text{m}$ .

### 2.4.2 Mesodermal Cell Movements

An exceedingly important event during amniote embryogenesis is the ingression of epiblastic cells through the primitive streak (Gilbert 2010). During ingression, mesenchymal cells migrate laterally and cranially in an ECM-rich environment. Thus, ingressing mesodermal cells represent, arguably, the premiere example of an embryonic mesenchymal cell population, in amniotes. Zamir et al. (2006) studied the newly ingressed mesodermal cells in HH stage 4 or 5 avian embryos. A portion of the ECM was labeled using microinjected fluorescently conjugated B3D6 antibodies specific for fibronectin. Mesodermal cells were tagged by lipophilic dyes (DiI), applied at the primitive streak. The apparent (total) displacements of labeled cells were manually determined. The ECM displacement field was determined by PIV analysis, and cell-autonomous displacements were obtained using relation (2.1).

In accord with Fig. 2.3, the ECM lateral to the primitive streak was found to move further laterally. Mesodermal cells move in the same direction but faster than the ECM; nevertheless, a substantial portion of the total cellular displacements is also displayed by the ECM. The study found an increasing cranial-to-caudal gradient in cell speed: Cells that emanate from more caudal (posterior) positions in the primitive streak move faster than cells closer to Hensen's node (more anterior). As mesodermal cells move away from the primitive streak, they slow down to speeds that match those of their local ECM scaffold. This change in

relative cell-to-ECM speed is believed to occur concomitantly with the mesenchymal (mesodermal) cells integrating to form a LPM, an epithelium. Note that the formation of the LPM occurs at positions anterior to the sites of cell ingression—again mainly due to tissue movements that result in the continuous regression of Hensen’s node. In other words, Hensen’s node has moved (caudally) and “passed” the newly forming LPM.

As shown in a recent study by Benazeraf et al. (2010), active motion of the mesenchymal cells, which comprise the pre-somitic mesoderm, is randomly directed. The intensity of mesenchymal cell motion gradually decreases at more anterior positions, at which time/place these cells condense into the pre-somitic mesoderm. Benazeraf and colleagues found, via cells expressing a dominant negative FGF receptor, that FGF signaling is a likely regulator of the intensity of active, randomly directed cellular motility.

These novel data shed new light on the classical cell fate-mapping studies of the mesoderm—it is now clear that for the most part, cells forming either the pre-somitic or the LPM move to their future positions by tissue-level rearrangements (shared by both the cells and the surrounding ECM environment) as opposed to individual cell, directed motile activity of individual cells, relative to the ECM.

### 2.4.3 *Endothelial Progenitor Movements*

Endothelial cells of the avian embryo originate as right and left subpopulations of the LPM and then dislocate ventrally into a prominent ECM layer situated between the endoderm and the mesoderm. During the ensuing process, that is, vasculogenesis, primordial endothelial cells assemble a primary vascular plexus within a relatively planar, sheet-like, ECM environment.

Endothelial cells can be tracked by use of microinjected and fluorochrome-conjugated QH1 antibodies, specific for quail vascular endothelium (Pardanaud et al. 1987; Rupp et al. 2004), or using the recently developed transgenic quail line in which endothelial nuclei express yellow fluorescent protein (YFP, Sato et al. 2010). In the Tg(tie1:H2B-eYFP) quail, a fusion between histone H2B and enhanced YFP is driven by the promoter of the TIE1 gene. Thus, transgenic embryos express H2B-eYFP in the nuclei of endothelial and endocardial precursor cells. TIE1+ nuclei are detectable at the earliest stages of vasculogenesis, approximately the same stage when the QH1 epitope appears (Sato et al. 2010).

At stage HH7 there is a substantial medial movement of the forming vascular plexus, a phenomenon predicted by Coffin and Poole (1988). This process, vascular drift, was shown to occur across the entire nascent vascular plexus (Rupp et al. 2004). Early vasculogenesis, however, occurs during a time of vigorous rearrangements in the embryo. In fact, the drift motion of vascular segments is largely coincident with that of the surrounding ECM (Czirok et al. 2008; Sato et al. 2010), an outcome which is to be expected if nascent vessels are embedded in a mechanical continuum. Counterintuitively, active endothelial cell movements at

the onset of vasculogenesis are largely random. Thus, although primordial endothelial cells are actively motile, the majority of their gross medial displacement at these stages is the consequence of medialward drift of the ECM scaffold.

#### **2.4.4 Endocardial Progenitor Movements**

Endocardial progenitors are also commonly assumed to migrate from their sites of differentiation in the LPM towards the midline (Gilbert 2010). Yet, as with mesenchymal cells and vascular endothelial progenitors, when endocardial progenitor cell motion is compared to that of the ECM environment, a large degree of similarity is found. In fact, the empirical data show that a distinct medial motion pattern is fully shared between the ECM and the future endocardial cell population. In contrast, the active motion of endocardial cells is randomly directed and of much smaller magnitude. The calculated autonomous speeds of 20  $\mu\text{m}/\text{h}$  are in the same range as those reported for endothelial cells moving in culture: 10  $\mu\text{m}/\text{h}$  by Szabo et al. (2010) and 50  $\mu\text{m}/\text{h}$  by Kouvroukoglou et al. (2000). By way of comparison, the active movement of gastrulating mesoderm cells is somewhat faster, in the range of 60  $\mu\text{m}/\text{h}$  (Zamir et al. 2006). Thus, four embryonic mesenchymal cell populations, newly ingressed mesodermal, pre-somitic, endothelial, and endocardial, exhibit similar random motile activity within the context of large-scale tissue (ECM) drift.

### **2.5 Perspectives**

The most likely interpretation for the shared large-scale movement pattern between ECM components (like fibronectin and fibrillin-2) and cells is a model whereby the whole tissue (cells and the associated ECM) moves as a composite material and deforms in response to mechanical forces. The recent finding that microinjected inert particles also translocate to the forming heart, in a manner identical to ECM fibrils (Aleksandrova et al. 2012), is entirely consistent with such a view. On the other hand, cells can actively remodel, pull, and drag the ECM. Therefore, our view that cells can move relative to a conveyor-belt-like ECM that largely contributes to their displacements is an oversimplification. However, it is equally difficult to envision overt, large-scale, relative displacements between tightly interwoven three-dimensional cellular elements and ECM scaffold elements. Furthermore, recent experiments revealed that in the case of an actively moving cell population, for example, vascular sprout cells, local ECM rearrangements accompanying cell invasion are negligible compared to the magnitude of the “rapid” fluctuating ECM motion, described above (Rupp et al. [In preparation](#)). Thus, for tissue-scale movements, the ECM indeed acts as an inert conveyor belt. On much smaller scales individual cells can slowly move and remodel the ECM.

The structure of the ECM, as a physical entity, is molded by mechanical stress (Keller et al. 2003). The best understood source of mechanical stress is cellular traction force (Stoplak and Harris 1982; Oliver et al. 1995), which was demonstrated to reorganize collagen filaments *in vitro* (Petroll and Ma 2003; Friedl and Wolf 2003). The mechanically driven ECM reorganization is often not reversible due to modifications in molecular configuration, which in turn enable chemical cross-linking or proteolysis (Wolf and Friedl 2005). In the case of fibronectin, for example, traction forces are needed to change the conformation of individual molecules and expose a cryptic binding site required for self-assembly (Zhong et al. 1998; Baneyx et al. 2001).

Lack of information regarding the motors driving the observed ECM (and tissue) movements remains a frustrating problem for developmental biologists and those interested in tissue mechanics (Chuai and Weijer 2009b). Future advances in the field depend on a better understanding of the material properties of the embryonic tissues and how they change over space and time. Knowledge about residual stresses within the tissue is essential to conclusively map the driving forces of tissue motion (Hutson et al. 2003, 2009; Varner et al. 2010).

The large-scale co-movement of cells and the surrounding ECM has implications for the establishment and maintenance of ECM-bound morphogen gradients as well (Chuai and Weijer 2009a). Fibronectin was shown to control the availability of growth factors such as TGFbeta (Fontana et al. 2005; Leiss et al. 2008) and can bind VEGF (Wijelath et al. 2002), in some cases acting in a synergistic manner with heparan sulfate (Stenzel et al. 2011). We predict that the observed substantial ECM movement is likely to deform the concentration fields of the secreted morphogens. Furthermore, as the ECM seems to be extensively reused during morphogenesis, morphogen gradients established at earlier time at some distinct region of the embryo may provide guidance cues at later time stages of development. On the other hand, if the secreted morphogen has a short lifetime, then the ECM displacements can have little bearing on the morphogen signaling. In short, ECM motion likely impacts the bioavailability of morphogen gradients.

Empirical time-lapse data and subsequent computational analysis of multiple prominent morphogenetic events all suggest that earlier studies overestimated the apparent degree of autonomous cell motility in bird embryos. While results regarding relative motion of cells and ECM cannot be simply extrapolated to the morphogenesis of other organs, the findings described in this chapter pose the possibility that what is true during gastrulation, vertebral axis elongation, vasculogenesis, and endocardial morphogenesis may also be true for other organs where mesoderm plays a morphogenetic role. The presented findings also beg the question of whether lessons learned about morphogenetic movements, in amniotes, can be directly translated to understanding morphogenesis in evolutionarily older vertebrates. Several tissue movements, such as the assembly of a heart from bilateral primordia secondary to formation of a foregut, have no direct counterparts in non-amniote vertebrates. Stated differently—due to the striking extent of their millimeter-scale tissue deformations—did morphogenetic strategies evolve in amniotes, which distinguish them from non-amniotes?



**Acknowledgments** This work was supported by the NIH R01 grants HL087136 (AC), HL085694 (BJR), HL068855 (CDL); the Hungarian Research Fund OTKA K72664 (AC); and the G. Harold & Leila Y. Mathers Charitable Foundation (AC, CDL, BJR).

## References

- Alberts B, Johnson A, Lewis J, Raff M, Roberts K, Walter P (2008) *Molecular Biology of the Cell*. Garland Science, New York
- Aleksandrova A, Czirok A, Szabo A, Filla M, Hossain J, Whelan P, Lansford R, Rongish B (2012) Convective tissue movements play a major role in avian endocardial morphogenesis. *Dev Biol* 363(2):348–361
- Aufschnaiter R, Zamir EA, Little CD, Ozbek S, Mnder S, David CN, Li L, Sarras MP, Zhang X (2011) In vivo imaging of basement membrane movement: Ecm patterning shapes hydra polyps. *J Cell Sci* 124:4027–4038. doi:[10.1242/jcs.087239](https://doi.org/10.1242/jcs.087239)
- Baneyx G, Baugh L, Vogel V (2001) Coexisting conformations of fibronectin in cell culture imaged using fluorescence resonance energy transfer. *Proc Natl Acad Sci USA* 98:14464–14468
- Barocas V, Tranquillo R (1997) An anisotropic biphasic theory of tissue-equivalent mechanics: the interplay among cell traction, fibrillar network deformation, fibril alignment, and cell contact guidance. *J Biomech Eng* 119(2):137–145
- Benazeraf B, Francois P, Baker RE, Denans N, Little CD, Pourquie O (2010) A random cell motility gradient downstream of fgf controls elongation of an amniote embryo. *Nature* 466:248–252. doi:[10.1038/nature09151](https://doi.org/10.1038/nature09151)
- Bertet C, Sulak L, Lecuit T (2004) Myosin-dependent junction remodelling controls planar cell intercalation and axis elongation. *Nature* 429:667–671. doi:[10.1038/nature02590](https://doi.org/10.1038/nature02590)
- Chuai M, Weijer CJ (2009a) Regulation of cell migration during chick gastrulation. *Curr Opin Genet Dev* 19:343–349. doi:[10.1016/j.gde.2009.06.007](https://doi.org/10.1016/j.gde.2009.06.007)
- Chuai M, Weijer CJ (2009b) Who moves whom during primitive streak formation in the chick embryo. *HFSP J* 3:71–76. doi:[10.2976/1.3103933](https://doi.org/10.2976/1.3103933)
- Coffin D, Poole T (1988) Embryonic vascular development: immunohistochemical identification of the origin and subsequent morphogenesis of the major vessel primordia in quail embryos. *Development* 102:735–748
- Cui C, Lansford R, Filla MB, Little CD, Cheuvront TJ, Rongish BJ (2006) Electroporation and EGFP labeling of gastrulating quail embryos. *Dev Dyn* 235:2802–2810. doi:[10.1002/dvdy.20895](https://doi.org/10.1002/dvdy.20895)
- Cui C, Little CD, Rongish BJ (2009) Rotation of organizer tissue contributes to left-right asymmetry. *Anat Rec (Hoboken)* 292:557–561. doi:[10.1002/ar.20872](https://doi.org/10.1002/ar.20872)
- Cukierman E, Pankov R, Stevens DR, Yamada KM (2001) Taking cell-matrix adhesions to the third dimension. *Science* 294:1708–1712
- Czirok A, Rupp P, Rongish B, Little C (2002) Multi-field 3D scanning light microscopy of early embryogenesis. *J Microsc* 206:209–217
- Czirok A, Rongish BJ, Little CD (2004) Extracellular matrix dynamics during vertebrate axis formation. *Dev Biol* 268:111–122. doi:[10.1016/j.ydbio.2003.09.040](https://doi.org/10.1016/j.ydbio.2003.09.040)
- Czirok A, Zach J, Kozel BA, Mecham RP, Davis EC, Rongish BJ (2006a) Elastic fiber macro-assembly is a hierarchical, cell motion-mediated process. *J Cell Physiol* 207:97–106. doi:[10.1002/jcp.20573](https://doi.org/10.1002/jcp.20573)
- Czirok A, Zamir EA, Filla MB, Little CD, Rongish BJ (2006b) Extracellular matrix macroassembly dynamics in early vertebrate embryos. *Curr Top Dev Biol* 73:237–258. doi:[10.1016/S0070-2153\(05\)73008-8](https://doi.org/10.1016/S0070-2153(05)73008-8)
- Czirok A, Zamir EA, Szabo A, Little CD (2008) Multicellular sprouting during vasculogenesis. *Curr Top Dev Biol* 81:269–289. doi:[10.1016/S0070-2153\(07\)81009-X](https://doi.org/10.1016/S0070-2153(07)81009-X)

- Dickinson RB, Guido S, Tranquillo RT (1994) Biased cell migration of fibroblasts exhibiting contact guidance in oriented collagen gels. *Ann Biomed Eng* 22:342–356
- Dubey N, Letourneau P, Tranquillo R (2001) Neuronal contact guidance in magnetically aligned fibrin gels: effect of variation in gel mechano-structural properties. *Biomaterials* 22(10):1065–1075
- Engler AJ, Sen S, Sweeney HL, Discher DE (2006) Matrix elasticity directs stem cell lineage specification. *Cell* 126:677–689. doi:[10.1016/j.cell.2006.06.044](https://doi.org/10.1016/j.cell.2006.06.044)
- Fontana L, Chen Y, Prijatelj P, Sakai T, Fessler R, Sakai LY, Rifkin DB (2005) Fibronectin is required for integrin  $\alpha$ 5 $\beta$ 1-mediated activation of latent TGF- $\beta$  complexes containing LTBP-1. *FASEB J* 19:1798–1808. doi:[10.1096/fj.05-4134com](https://doi.org/10.1096/fj.05-4134com)
- Friedl P, Wolf K (2003) Tumour-cell invasion and migration: diversity and escape mechanisms. *Nat Rev Cancer* 3(5):362–374
- Gardner JM, Fambrough DM (1983) Fibronectin expression during myogenesis. *J Cell Biol* 96:474–485
- Gilbert SF (2010) *Developmental Biology*, 9th edn. Sinauer Associates, Inc., Sunderland, MA
- Gros J, Feistel K, Viebahn C, Blum M, Tabin CJ (2009) Cell movements at hensen's node establish left/right asymmetric gene expression in the chick. *Science* 324:941–944. doi:[10.1126/science.1172478](https://doi.org/10.1126/science.1172478)
- Gumbiner BM (2005) Regulation of cadherin-mediated adhesion in morphogenesis. *Nat Rev Mol Cell Biol* 6:622–634. doi:[10.1038/nrm1699](https://doi.org/10.1038/nrm1699)
- Hamburger V, Hamilton H (1951) A series of normal stages in the development of the chick embryo. *J Morphol* 88:49–92
- Hutson MS, Tokutake Y, Chang MS, Bloor JW, Venakides S, Kiehart DP, Edwards GS (2003) Forces for morphogenesis investigated with laser microsurgery and quantitative modeling. *Science* 300:145–149. doi:[10.1126/science.1079552](https://doi.org/10.1126/science.1079552)
- Hutson MS, Veldhuis J, Ma X, Lynch HE, Cranston PG, Brodland GW (2009) Combining laser microsurgery and finite element modeling to assess cell-level epithelial mechanics. *Biophys J* 97:3075–3085. doi:[10.1016/j.bpj.2009.09.034](https://doi.org/10.1016/j.bpj.2009.09.034)
- Keller R, Davidson LA, Shook DR (2003) How we are shaped: the biomechanics of gastrulation. *Differentiation* 71:171–205
- Kouvroukoglou S, Dee KC, Bizios R, McIntire LV, Zygourakis K (2000) Endothelial cell migration on surfaces modified with immobilized adhesive peptides. *Biomaterials* 21:1725–1733
- Kozel BA, Rongish BJ, Czirok A, Zach J, Little CD, Davis EC, Knutsen RH, Wagenseil JE, Levy MA, Mecham RP (2006) Elastic fiber formation: a dynamic view of extracellular matrix assembly using timer reporters. *J Cell Physiol* 207:87–96. doi:[10.1002/jcp.20546](https://doi.org/10.1002/jcp.20546)
- Lauffenburger DA, Horwitz AF (1996) Cell migration: a physically integrated molecular process. *Cell* 84:359–369
- Leiss M, Beckmann K, Girs A, Costell M, Fessler R (2008) The role of integrin binding sites in fibronectin matrix assembly in vivo. *Curr Opin Cell Biol* 20:502–507. doi:[10.1016/j.ceb.2008.06.001](https://doi.org/10.1016/j.ceb.2008.06.001)
- Little C, Drake C (2000) Whole-mount immunolabeling of embryos by microinjection. *Methods Mol Biol* 135:183–189
- Martin AC, Kaschube M, Wieschaus EF (2009) Pulsed contractions of an actin-myosin network drive apical constriction. *Nature* 457:495–499. doi:[10.1038/nature07522](https://doi.org/10.1038/nature07522)
- Montell DJ (2008) Morphogenetic cell movements: diversity from modular mechanical properties. *Science* 322:1502–1505. doi:[10.1126/science.1164073](https://doi.org/10.1126/science.1164073)
- Oliver T, Dembo M, Jacobson K (1995) Traction forces in locomoting cells. *Cell Motil Cytoskeleton* 31(3):225–240
- Olsen L, Maini P, Sherratt J, Dallon J (1999) Mathematical modelling of anisotropy in fibrous connective tissue. *Math Biosci* 158:145–170
- Pardanaud L, Altmann C, Kitos P, Dieterlen-Lievre F, Buck C (1987) Vasculogenesis in the early quail blastodisc as studied with a monoclonal antibody recognizing endothelial cells. *Development* 100:339–349

- Petroll WM, Ma L (2003) Direct, dynamic assessment of cell-matrix interactions inside fibrillar collagen lattices. *Cell Motil Cytoskeleton* 55:254–264
- Ridley AJ, Schwartz MA, Burridge K, Firtel RA, Ginsberg MH, Borisy G, Parsons JT, Horwitz AR (2003) Cell migration: integrating signals from front to back. *Science* 302:1704–1709. doi:[10.1126/science.1092053](https://doi.org/10.1126/science.1092053)
- Rongish B, Drake C, Argraves W LC (1998) Identification of the developmental marker, JB3-antigen, as fibrillin-2 and its de novo organization into embryonic microfibrillar arrays. *Dev Dyn* 212:461–471
- Rozario T, DeSimone DW (2010) The extracellular matrix in development and morphogenesis: a dynamic view. *Dev Biol* 341:126–140. doi:[10.1016/j.ydbio.2009.10.026](https://doi.org/10.1016/j.ydbio.2009.10.026)
- Rupp PA, Czirok A, Little CD (2004)  $\alpha$ v $\beta$ 3 integrin-dependent endothelial cell dynamics in vivo. *Development* 131:2887–2897
- Rupp P, Szabo A, Kosa E, Czirok A (manuscript in preparation) Fibronectin dynamics during vasculogenesis
- Sato Y, Poynter G, Huss D, Filla MB, Czirok A, Rongish BJ, Little CD, Fraser SE, Lansford R (2010) Dynamic analysis of vascular morphogenesis using transgenic quail embryos. *PLoS One* 5:e12674. doi:[10.1371/journal.pone.0012674](https://doi.org/10.1371/journal.pone.0012674)
- Sivakumar P, Czirok A, Rongish BJ, Divakara VP, Wang YP, Dallas SL (2006) New insights into extracellular matrix assembly and reorganization from dynamic imaging of extracellular matrix proteins in living osteoblasts. *J Cell Sci* 119:1350–1360. doi:[10.1242/jcs.02830](https://doi.org/10.1242/jcs.02830)
- Stenzel D, Lundkvist A, Sauvaget D, Busse M, Graupera M, van der Flier A, Wijelath ES, Murray J, Sobel M, Costell M, Takahashi S, Fessler R, Yamaguchi Y, Gutmann DH, Hynes RO, Gerhardt H (2011) Integrin-dependent and -independent functions of astrocytic fibronectin in retinal angiogenesis. *Development* 138:4451–4463. doi:[10.1242/dev.071381](https://doi.org/10.1242/dev.071381)
- Stoplak D, Harris A (1982) Connective tissue morphogenesis by fibroblast traction. *Dev Biol* 90:383–398
- Szabo A, Unnep R, Mehes E, Twal WO, Argraves WS, Cao Y, Czirok A (2010) Collective cell motion in endothelial monolayers. *Phys Biol* 7:046007. doi:[10.1088/1478-3975/7/4/046007](https://doi.org/10.1088/1478-3975/7/4/046007)
- Szabo A, Rupp PA, Rongish BJ, Little CD, Czirok A (2011) Extracellular matrix fluctuations during early embryogenesis. *Phys Biol* 8:045006. doi:[10.1088/1478-3975/8/4/045006](https://doi.org/10.1088/1478-3975/8/4/045006)
- Tomasek JJ, Hay ED, Fujiwara K (1982) Collagen modulates cell shape and cytoskeleton of embryonic corneal and fibroblast fibroblasts: distribution of actin, alpha-actinin, and myosin. *Dev Biol* 92:107–122
- Varner VD, Voronov DA, Taber LA (2010) Mechanics of head fold formation: investigating tissue-level forces during early development. *Development* 137:3801–3811. doi:[10.1242/dev.054387](https://doi.org/10.1242/dev.054387)
- Vasiev B, Balter A, Chaplain M, Glazier JA, Weijer CJ (2010) Modeling gastrulation in the chick embryo: formation of the primitive streak. *PLoS One* 5:e10571. doi:[10.1371/journal.pone.0010571](https://doi.org/10.1371/journal.pone.0010571)
- Vernon R, Lara S, Drake C, Iruela-Arispe M, Angello J, Little C, Wight T, Sage E (1995) Organized type I collagen influences endothelial patterns during “spontaneous angiogenesis in vitro”: planar cultures as models of vascular development. *In Vitro Cell Dev Biol Anim* 31(3):120–131
- Wijelath ES, Murray J, Rahman S, Patel Y, Ishida A, Strand K, Aziz S, Cardona C, Hammond WP, Savidge GF, Rafii S, Sobel M (2002) Novel vascular endothelial growth factor binding domains of fibronectin enhance vascular endothelial growth factor biological activity. *Circ Res* 91:25–31
- Wolf K, Friedl P (2005) Functional imaging of pericellular proteolysis in cancer cell invasion. *Biochimie* 87:315–320
- Yang X, Dormann D, Munsterberg A, Weijer C (2002) Cell movement patterns during gastrulation in the chick are controlled by positive and negative chemotaxis mediated by FGF4 and FGF8. *Dev Cell* 3:425–437

- Zamir E, Katz BZ, Aota S, Yamada KM, Geiger B, Kam Z (1999) Molecular diversity of cell-matrix adhesions. *J Cell Sci* 112(Pt 11):1655–1669
- Zamir EA, Czirok A, Rongish BJ, Little CD (2005) A digital image-based method for computational tissue fate mapping during early avian morphogenesis. *Ann Biomed Eng* 33:854–865
- Zamir EA, Czirok A, Cui C, Little CD, Rongish BJ (2006) Mesodermal cell displacements during avian gastrulation are due to both individual cell-autonomous and convective tissue movements. *Proc Natl Acad Sci USA* 103:19806–19811
- Zhong C, Chrzanowska-Wodnicka M, Brown J, Shaub A, Belkin AM, Burridge K (1998) Rhomediates contractility exposes a cryptic site in fibronectin and induces fibronectin matrix assembly. *J Cell Biol* 141:539–551



<http://www.springer.com/978-3-642-35934-7>

Extracellular Matrix in Development

DeSimone, D.W.; Mecham, R. (Eds.)

2013, X, 253 p., Hardcover

ISBN: 978-3-642-35934-7